ELSEVIER

Journal of Magnetism and Magnetic Materials 175 (1997) 237–248

Journal of magnetism and magnetic materials

Study of domain structure of thin magnetic films by polarised neutron reflectometry

V.M. Pusenkov*, N.K. Pleshanov, V.G. Syromyatnikov, V.A. Ul'yanov, A.F. Schebetov

Petersburg Physics Institute, PNPI, 188350 Gatchina, Leningrad, St-Petersburg, Russia

Received 17 March 1997; received in revised form 23 June 1997

Abstract

A technique based on specular reflection of polarised neutrons, complemented by polarisation analysis and small-angle (diffuse) scattering under reflection has been suggested for determination of parameters of domain structure of thin (~ 10–10^3 nm) films. The generalised matrix formalism developed to cope with the problem of reflection of neutrons from layered magnetic media with magnetisation arbitrary in magnitude and direction allowed to describe the specular reflection from unmagnetised films. It has been shown that under total reflection the local (averaged over the region coherently illuminated by a neutron) magnetic induction, the mean (averaged over the sample) magnetic induction and the mean square direction cosines of the magnetic induction enter into the reflection and depolarisation matrices. It has also been shown that the first two Fourier transform coefficients of the angular distribution function of the domain magnetisation, connected with the mean magnetisation and magnetic texture, can be experimentally found. The study of magnetisation processes in $Fe_{36}Co_{64}$ (170 ± 3 nm) and Co (110 ± 3 nm) films demonstrates the possibilities of the new technique. The optical effect of averaging over the region coherently illuminated by a neutron, effectively leading to a decrease in the 'local' measured magnetic induction of the Co film, has been observed for the first time.

PACS: 61.12.Ha; 75.60. – d

Keywords: Domains; Polarization analysis; Reflectometry; Thin films

1. Introduction

Several techniques used to study the domain structure of ferromagnetic materials are known at present. First of all, the well-developed powder pattern technique is to be mentioned. The magneto-optical techniques based on rotation of the polarisation plane of light, both under transmission (the Faraday effect) and under reflection (the Kerr effect), are also widely used. Polarised neutron techniques have also been found useful in this research field. The parameters of the domain structure are determined in neutron transmission experiments by measuring the polarisation of the beam traversing the sample (depolarisation analysis) and in small-angle neutron scattering (SANS).

* Corresponding author. Tel.: + 7 812 71 46973; fax: + 7 812 71 39053; e-mail: pusenkov@lnpi.spb.su.

PII S0304-8853(97)00247-3

The theory of depolarisation of neutrons traversing a bulk sample has been founded by Halpern and Holstein [1] and developed in papers [2–8]. Measuring the change in the neutron beam polarisation, one can determine the mean square direction cosines of the magnetic induction, the size of magnetic inhomogeneities (mean domain size, correlation length), and the mean magnetisation. In order to obtain measurable depolarisation effects and find these parameters for thin films, their total thickness is increased, e.g. by piling the thin films up into a stack [9].

Small-angle neutron-scattering technique has been for quite a long time used to study magnetic inhomogeneities in bulk samples. Multiple refraction of neutrons at the domain walls which gives rise to small-angle neutron scattering is informative about the mean domain size. More detailed information about the domain wall structure may be obtained by measuring refraction of neutrons at single-domain boundaries using SANS instruments [10] or double-crystal spectrometers [11–13]. It is to be noted that small-angle scattering under reflection of neutrons from domain structure of ferromagnetic films has been observed earlier [14], and the characteristic parameters of the magnetic inhomogeneities have been thus evaluated.

Polarised neutron reflectometry (PNR) [15] is a powerful technique which can be used to study quite complicated magnetic structures [16–21]. It enables one to get information about the state of interfacial regions including roughness and interdiffusion [22], to determine the thicknesses of a thin-film structure and oxidation of the topmost layers, etc.

In the present work the possibilities of PNR are suggested for the study of domain structure of thin films. The proposed technique is based on specular reflection of polarised neutrons, complemented by polarisation analysis and small-angle (diffuse) scattering under reflection from demagnetised magnetic films. It has been shown that the local (averaged over the region coherently illuminated by the neutron) magnetic induction, the mean (averaged over the sample) magnetic induction and the mean square direction cosines of the magnetic induction can be additionally found for thin (~ 10–10^3 nm) films. Investigation of such thin films is of considerable interest, since they become widely used in magnetic memory devices. The possibilities of the technique have been demonstrated by the study of magnetisation processes in $Fe_{36}Co_{64}$ (170 ± 3 nm) and Co (110 ± 3 nm) films prepared by magnetron sputtering and electron beam evaporation techniques, respectively.

2. Theory

When a film is in a demagnetised state, the regions of spontaneous magnetisation (domains) are, as a rule, not collinear to the polarisation vector of the incident neutrons. A series of interesting phenomena can be observed when neutrons are reflected from such a demagnetised film, including rotation of the polarisation vector under reflection, small-angle (diffuse) scattering at domains, and depolarisation of the reflected beam. The formalism developed in [21, 23, 24], where reflection of neutrons from layered magnetic media with magnetisation arbitrary in magnitude and direction is treated, allowed to describe the specular reflection from unmagnetised films.

Consider first reflection of neutrons from a single domain. The potentials of a magnetic film on glass for two spin components, up and down the magnetic field in the film ($\boldsymbol{B}$), $V^{\pm} = V_N \pm V_M$ (V_N and V_M are its nuclear and magnetic potentials) are represented in Fig. 1. The y-axis is normal to the

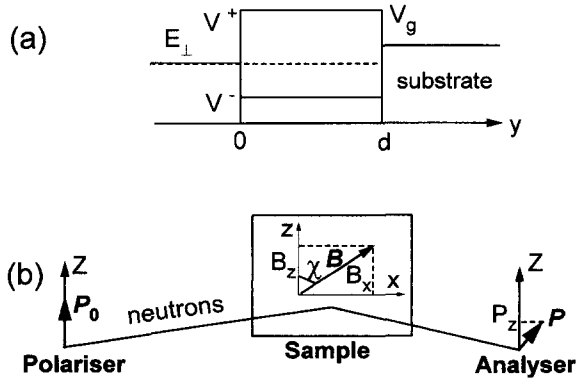

Fig. 1. (a) The potentials of a magnetic film. (b) The experimental scheme. The directions of the quantisation axis (Z), the guide field ($\boldsymbol{H}$), and the magnetic induction in the film ($\boldsymbol{B}$) are shown; the coordinate system (x, y, z) is connected with the sample.

sample surface, and the z-axis is parallel to the guide field $\boldsymbol{H}$. The quantisation axis Z is chosen to be parallel to $\boldsymbol{H}$ and collinear with the incident beam polarisation $\boldsymbol{P}_0$, χ is the angle between $\boldsymbol{H}$ and $\boldsymbol{B}$ (both are assumed to be 'in-plane'). It can be shown [21] that, in the approximation of weak guide fields, the reflection matrix r' is diagonal in the coordinate system with a quantisation axis $Z' \| \boldsymbol{B}$, r'_{++} and r'_{--} being reflection Fresnel amplitudes for neutrons with the spin 'up' (+) and 'down' (−) $\boldsymbol{B}$. Using the unitary transformation from one system of coordinates to another, one can find the reflection matrix in the coordinate system with $Z \| \boldsymbol{H}$ [21]:

$$r_{-+} = r_{+-} = \tfrac{1}{2}(r'_{--} - r'_{++}) \sin(\chi), \tag{1a}$$

$$r_{++} = r'_{++} \cos^2(\chi/2) + r'_{--} \sin^2(\chi/2). \tag{1b}$$

For the sake of simplicity, consider only the case of total reflection: $E_\perp < V_g$, when $r'_{++} = \exp(i\varphi_+)$ and $r'_{--} = \exp(i\varphi_-)$. As a result of reflection, the polarisation vector will be rotated about $\boldsymbol{B}$:

$$\boldsymbol{P} = D(\boldsymbol{n}, \varphi)\, \boldsymbol{P}_0, \tag{2}$$

where $D(\boldsymbol{n}, \varphi)$ is the matrix of rotation about $\boldsymbol{n} = \boldsymbol{B}/B$ by an angle φ. The angle of rotation of the polarisation vector, $\varphi = \varphi_+ - \varphi_-$, is determined by the phase shifts of the opposite spin components, up and down the field $\boldsymbol{B}$ [25]

$$\varphi_+ = 2 \arccos\{[E_\perp / V^+]^{1/2}\} \quad (E_\perp < V^+), \tag{3a}$$

$$\varphi_- = 2 \arccos\{[E_\perp / V_g]^{1/2}\} + 2k_\perp d \quad (V^- < E_\perp < V_g). \tag{3b}$$

The term $2k_\perp d$ is due to the fact that, unlike the (+) spin component, the (−) spin component is reflected at the boundary 'film/substrate' (Fig. 1a). Since $R^+ = R_{-+} + R_{++} = 1$, the Z-projection of the polarisation vector takes the following form:

$$P_z = D_{zz}(\boldsymbol{n}, \varphi) = 2R_{++} - 1 = 1 - n_x^2 (1 - \cos(\varphi)). \tag{4}$$

It follows from Eq. (4) that in the given case the flipping is complete ($P_z = -1$) when

$$\boldsymbol{B} \perp \boldsymbol{H} (\chi = \pi/2) \quad \text{and} \quad \varphi = \pi(1 + 2N), \tag{5}$$

where $N = 0, 1, 2, 3 \cdots$.

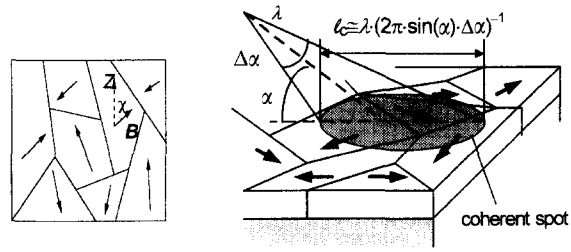

Fig. 2. The domain structure of a magnetic film and the neutron coherent illumination length l_c.

On the other hand, neutrons are reflected without spin-flipping ($P_z = 1$) when

$$\varphi = 2\pi N. \tag{6}$$

It is worth noting that similar processes take place under reflection of neutrons from layered periodic structures with AFM ordering [26]. One magnetic structure with a period $2L$ is then shifted with respect to the other by L. In the 'magnetic' diffraction order of reflection ($k_\perp = \pi/2L$), when the angle $\varphi = 2k_\perp L = \pi$, all neutrons are reflected with spin flipping, whereas in the 'structural' order ($k_\perp = \pi/L$), they are reflected without spin flipping.

Using the statistical approach [1, 5], one can introduce the angular distribution function $f(\chi)$ of the domain magnetisation (Fig. 2) and calculate the neutron reflectivities averaged over the sample. Therefore, in the region of total reflection, one has to go from the rotation matrix to the depolarisation matrix $D = \langle D(\boldsymbol{n}, \varphi) \rangle$. Accordingly, it follows from Eq. (4) that

$$P_z = D_{zz} = \langle 1 - n_x^2 (1 - \cos(\varphi)) \rangle. \tag{7}$$

The following quantities can be then defined [5]:

$$m_z \equiv \langle n_z \rangle = \langle f(\chi) \cos(\chi) \rangle = \langle B_z \rangle / B, \tag{8a}$$

$$\gamma_x \equiv \langle n_x^2 \rangle = (1 - \langle f(\chi) \cos(2\chi) \rangle)/2. \tag{8b}$$

Here m_z is the z-component of the reduced mean induction, and γ_x is the mean square direction cosines of the magnetic induction of domains. Note that the spin-up reflectivity and the Z-projection of the polarisation vector of the reflected beam in the region of the 'normal' energies $E_\perp < V^+$, provided that the spin component antiparallel to $\boldsymbol{B}$ is weakly reflected, i.e. $|r'_{--}| \ll |r'_{++}| \cong 1$,

are accordingly

$$R^{+} = R_{-+} + R_{++} \cong \langle \cos^2(\chi/2) \rangle = \tfrac{1}{2}(1 + m_z), \quad (9a)$$

$$P_z \cong 1 - \tfrac{1}{2} \langle \sin^2(\chi) \rangle \langle \cos^{-2}(\chi/2) \rangle$$

$$= 1 - \gamma_x/(1 + m_z). \quad (9b)$$

When averaging over domains, one has to take account of the relation between the domain size δ and the coherent illumination length $l_c \cong 1/\Delta k_{\|}$, connected with the uncertainty relation for the neutron wave-number component parallel to the surface, $\Delta k_{\|}$. It can be shown [27] that

$$l_c \cong \lambda\,(2\pi \sin(\alpha)\,\Delta\alpha)^{-1}, \quad (10)$$

where α is the glancing angle and $\Delta\alpha$ is the beam divergence.

Neutrons can be considered to be reflected from single domains when $\delta \gg l_c$. Then the relative phase shift φ, which depends not on the orientation of the magnetic induction but on its magnitude, is the same at any point of the sample. For reflection from a single domain, $\langle |\boldsymbol{B}| \rangle = B_s$, where B_s is the saturation induction.

The depolarisation matrix can be represented as [6]

$$D = \hat{I} + \langle \hat{A} \rangle \sin(\varphi) + \langle \hat{A}^2 \rangle (1 - \cos(\varphi)), \quad (11)$$

where $\hat{I}$ is the unit matrix and

$$\hat{A} = \begin{bmatrix} 0 & -n_z & 0 \\ n_z & 0 & -n_x \\ 0 & n_x & 0 \end{bmatrix}. \quad (12)$$

Measuring the depolarisation matrix D, one can find

$$m_z = (D_{yx} - D_{xy})/(2 \sin(\varphi)), \quad (13a)$$

$$\langle n_x \rangle = (D_{zy} - D_{yz})/(2 \sin(\varphi)), \quad (13b)$$

$$\cos(\varphi) = 1 - (\mathrm{Trace}(D) - 3)/2, \quad (13c)$$

$$\langle n_i^2 \rangle = 1 - (D_{ii} - 1)/(1 - \cos(\varphi)), \quad (13d)$$

where $i = x, z$,

$$\langle n_x n_z \rangle = \langle n_z n_x \rangle = \tfrac{1}{2}(D_{xz} + D_{zx})/(1 - \cos(\varphi)). \quad (13e)$$

As a result of total reflection, the polarisation vector is rotated about the vector $\langle \boldsymbol{n} \rangle = \langle \boldsymbol{B} \rangle / B$, and depolarisation is defined by the deviations of the magnetic induction directions of domains, $\Delta \boldsymbol{n}(z, y) = \boldsymbol{n}(z, y) - \langle \boldsymbol{n} \rangle$, from the mean direction. The spins of neutrons reflected at different parts of the mirror are rotated about different directions but on the same angle φ. Therefore, if condition (6) is satisfied, the beam polarisation after reflection will be unchanged.

When $\delta \leqslant l_c$, the local magnetic induction $\langle |\boldsymbol{B}| \rangle$ will be less than the saturation induction B_s, as a consequence of coherent averaging over different domains. At different parts of the sample, the local magnetic induction $|\boldsymbol{B}(z, x)|$ will be different, and the neutron spin will be rotated on different angles $\varphi(z, x) = \langle \varphi(z, x) \rangle + \Delta\varphi(z, x)$. The latter leads to an additional mechanism of depolarisation of the reflected neutron beam. It is evident that even when $\langle \varphi \rangle = 2\pi N$, the reflected beam will be (partly) depolarised. If $N > 1$ and the film is demagnetised, one may suggest that, when a domain boundary happens to be inside the coherent illumination region, $\Delta\varphi(z, x)$ may exceed 2π. Then the mean domain size can be found from

$$D_{zz} \sim (1 - \gamma_x l_c/\delta) \quad \text{when } \langle \varphi \rangle = 2\pi N. \quad (14)$$

Formula (14) allows one to evaluate the mean size of large ($\delta > l_c$) domains from depolarisation at points $\langle \varphi \rangle = 2\pi N$ in the region of total reflection. Using the spectral oscillating behaviour of P_z at a fixed glancing angle, one can determine the magnitude of the local magnetic induction $\langle |\boldsymbol{B}| \rangle$.

The condition $\delta < l_c$ corresponds to that for observation of diffraction at domains (Fig. 3). Additional information about the surface microstructure can be obtained from the intensity of diffuse scattering [28–31]. Formulas describing the intensity of diffuse scattering at island structures [29, 30] can be reformulated for the case of scattering at domain structures. In the simple case when magnetisation in all domains is collinear to the guide field, the intensity of diffuse scattering can be written in the Born approximation as

$$S_{\mathrm{diff}}(\boldsymbol{q}) \sim [\sin^2(q_\perp d/2)/q_\perp^2] K(q_{\|}), \quad (15)$$

where $\boldsymbol{q} = \boldsymbol{k} - \boldsymbol{k}'$ is the momentum transfer, $K(q_{\|})$ is the Fourier transform of the domain size correlation function related to the probability of crossing over from one domain to another, which can be

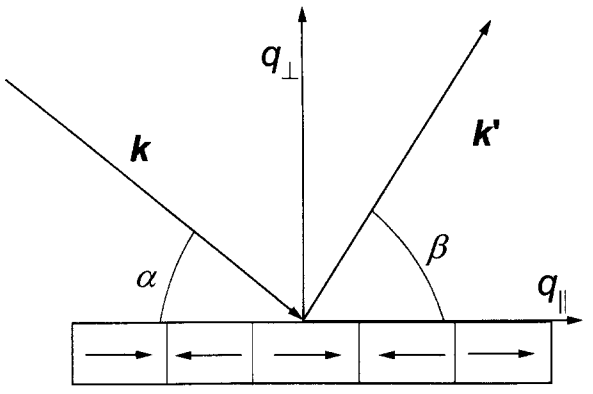

Fig. 3. A scheme of neutron scattering at the domain structure of a magnetic film. $\boldsymbol{q} = \boldsymbol{k} - \boldsymbol{k}'$ is the momentum transfer.

found from the transverse diffuse scans ($q_\perp$ = const).

Using one-dimensional polarisation analysis (Fig. 1), one can find the quantities m_z and γ_x connected (8) with the first two cosine coefficients of the Fourier transform of $f(\chi)$. It is to be noted that, rotating the sample about the surface normal in zero field, one can get more detailed information about the magnetic texture and the mean magnetic induction. Thus, rotating the sample by $\pi/2$, one obtains the first Fourier transform coefficient of $f(\chi)$: $m\exp(i\phi_m)$, where

$$m = (m_z^2 + m_x^2)^{1/2} = |\langle \boldsymbol{B} \rangle|/B,$$

$$\phi_m = \mathrm{arctg}(m_x/m_z) \tag{16}$$

and rotating by $\pi/4$, one obtains the second Fourier transform coefficient of $f(\chi)$: $\tau\exp(i\phi_\tau)$, where

$$\tau = [\langle f(\chi)\sin(2\chi)\rangle^2 + \langle f(\chi)\cos(2\chi)\rangle^2]^{1/2}, \tag{17a}$$

$$\phi_\tau = \mathrm{arctg}[\langle f(\chi)\sin(2\chi)\rangle / \langle f(\chi)\cos(2\chi)\rangle]. \tag{17b}$$

The quantity m determines the mean magnetisation of the sample and varies from 0 (demagnetised state) to 1 (magnetic saturation), and the angle $\phi_m \in [0, 2\pi]$ determines the mean magnetic induction direction in the film. The parameter τ defines the degree of magnetic texture of the film, which can change from 0 (isotropic state) to 1 (anisotropic state), and $\phi_\tau \in [0, \pi]$ determines the direction of the anisotropy axis. Applying the 3D polarisation analysis, all these quantities can be found from Eqs. (11)–(13) without rotation of the sample, since m enters into the matrix $\langle \hat{A} \rangle$ via m_x and m_z, and the texture parameter τ enters into the matrix $\langle \hat{A}^2 \rangle$ via

$$\gamma_x \equiv \langle n_x^2 \rangle = (1 - \langle f(\chi)\cos(2\chi)\rangle)/2, \tag{18a}$$

$$\langle n_x n_z \rangle = \langle f(\chi)\sin(\chi)\cos(\chi)\rangle = \tfrac{1}{2}\langle f(\chi)\sin(2\chi)\rangle. \tag{18b}$$

3. The experimental set-up

The present work has been carried out in Gatchina (Russia) at the reflectometer [27] supplemented with an analyser (Fig. 4). A polarised beam with neutrons of wavelengths $\lambda = 0.1$–0.4 nm (Fig. 5), cross-section $0.15 \times 30\ \mathrm{mm}^2$ and divergence 0.2 mrad is formed by a polarising neutron guide on the basis of the FeCo coating and by two slits, 1 and 2 (Fig. 4). The polarisation is analysed with a FeCo/TiZr supermirror. The flipper reverses the neutron spins adiabatically with respect to the vertical guide field formed by stray fields of the polariser and the sample electromagnet. It has been found out that the neutron spins adiabatically follow the guide field from the polariser to the analyser only when the magnetic field in the sample region exceeds 25 Oe (the maximum field available is 500 Oe). In all the experiments the applied field was parallel to the sample surface. The time-of-flight measurements of non-spin-flip (R_{++}) and spin-flip (R_{-+}) reflectivities were carried out with the flipper turned off and on, accordingly. Since $R_{+-} = R_{-+}$, the spin-up reflectivity $R^+ = R_{++} + R_{+-}$ and the Z-component of the corresponding polarisation vector $P_z = (R_{++} - R_{+-})\cdot(R_{++} + R_{+-})^{-1}$ can be calculated. Removing the

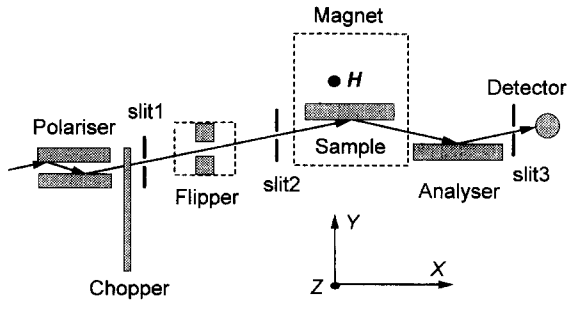

Fig. 4. A scheme of the neutron reflectometer ZINA.

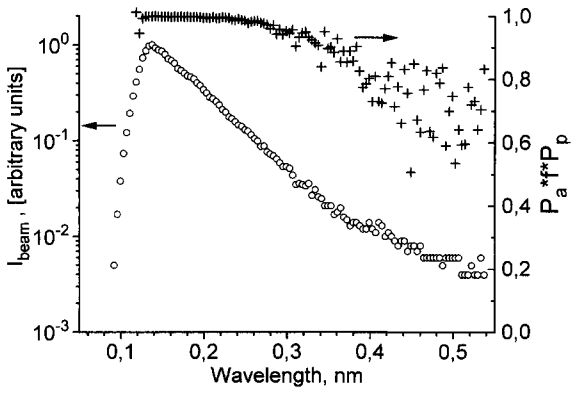

Fig. 5. The spectrum of the incident polarised neutron beam (I_{beam}) and the spectral dependence of the product of the efficiencies of the polariser, flipper and analyser ($P_p f P_a$).

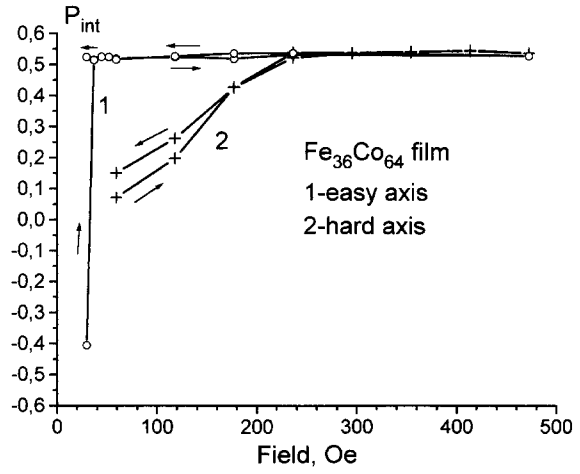

Fig. 6. The quantity P_{int} measured for a $Fe_{36}Co_{64}$ film as a function of the field applied along the easy (1) and hard (2) axes.

analyser, we measured also the quantity $P_{int} = (I_+ - I_-)\cdot(I_+ + I_-)^{-1}$ where I_+ and I_- are the integral intensities, accordingly, for the spin-up and spin-down neutron beams reflected from the sample. Measurements of small-angle (diffuse) scattering under reflection were carried out by scanning with the detector, the thin slit 3 (Fig. 4) having been attached. The coherent illumination region length (10) is changed in experiments with, e.g. the Co film ($\alpha = 2.5$ mrad) as a function of the wavelength from 30 μm at $\lambda = 0.1$ nm to 120 μm at $\lambda = 0.4$ nm.

The generalised matrix formalism developed to cope with the problem of reflection of neutrons from layered magnetic media with magnetisation arbitrary in magnitude and direction was used to fit the experimental data. The beam divergence and the spectral dependence of the product of the efficiences of the polariser, flipper and analyser, $P_p f P_a$ (Fig. 5), as well as the reflectivity of the analyser were taken into account. The model in Fig. 1, supplemented by an oxide layer, was used in data fitting.

4. $Fe_{36}Co_{64}$ film

For a $Fe_{36}Co_{64}$ film, prepared by magnetron sputtering, the quantity P_{int} was first measured (Fig. 6) as a function of the field applied both along the easy (1) and hard (2) axes. Further, the intensities at different detector positions β (see Fig. 3) and the spectral behaviour of P_z and R^+ (Figs. 8 and 9) were measured for a fixed glancing angle $\alpha = 3.7$ mrad. The coherent illumination region length is changed as a function of the wavelength from 20 to 80 μm.

From the fact that the diffuse wings and the width of the the specular peak are practically independent of the applied field (Fig. 7), one may conclude that neutrons are scattered at domains with dimensions by far exceeding 100 μm. The results of fitting of other parameters of the domain structure of the film in the field applied along the hard axis are tabulated in Fig. 8. When the field grows from 59 to 472 Oe, the film is being magnetised (m_z changes from 0.08 to 1.00), as can be directly seen in that region of the 'normal' energies $E_\perp < V^+$ where the spin component antiparallel to $\boldsymbol{B}$ is still weakly reflected (see Fig. 9). A monotonous decrease of γ_x from 0.86 to 0.00 testifies to the fact that there is a rotation of magnetisation. One may conclude from analysis of the parameters m_z and γ_x that the rotation is accompanied by movements of domain boundaries. It is to be noted that, when the film is almost completely ($m_z = 0.08$) demagnetised, the magnetisation of domains is oriented mainly ($\gamma_x = 0.86$) along the anisotropy axis ($\gamma_x = 0.5$ when $f(\chi)$ is isotropic), and under total reflection the quantity $P_z = 1 - \gamma_x(1 - \cos\varphi)$ is negative at

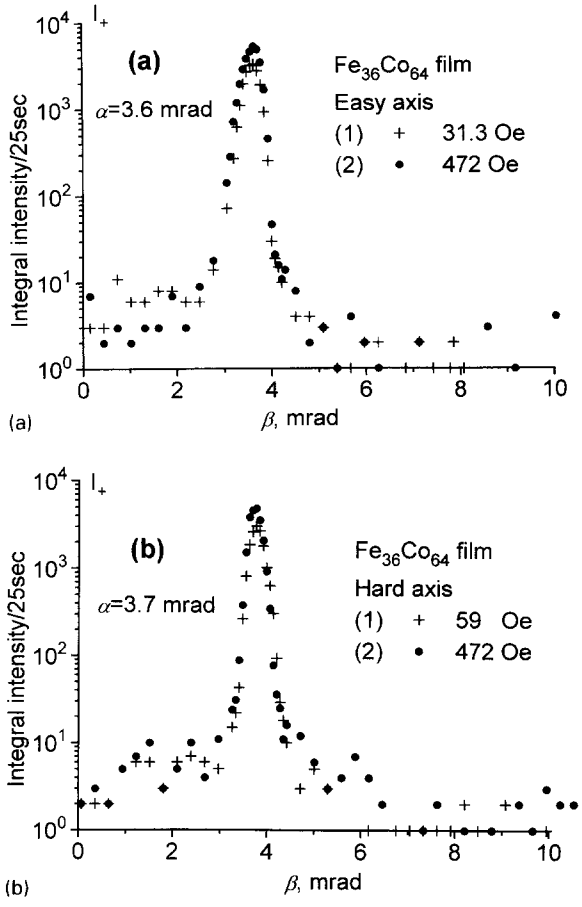

Fig. 7. The intensity I_+ of neutrons scattered from the demagnetised (curve 1) and magnetised (curve 2) $Fe_{36}Co_{64}$ film as a function of the scattering angle β. The field is applied along either the easy (a) or the hard (b) axis.

$\varphi = \pi(1 + 2N)$, in full agreement with the experiment (Fig. 8). The local magnetic induction is not changed during magnetisation (the positions of extrema of P_z are not changed) and is fitted to 19.1 kG. At $H = 472$ Oe the film is completely magnetised ($m_z = 1.0$ and $\gamma_x = 0.00$). When the field is reduced to 59 Oe, the film is partly demagnetised (m_z drops from 1 to 0.26). It may be concluded that the reversal of domain magnetisation (γ_x gradually increases from 0 to 0.86) is accompanied by movements of domain boundaries.

The reversal of magnetisation of the film with the easy axis parallel to the applied field is rapid ($m_z = -0.4$ at $H = 29.5$ Oe and $m_z = 1.0$ at $H = 44.3$ Oe). The domains remain to be collinear to the anisotropy axis ($\gamma_x \leqslant 0.03$). It means that the magnetisation process is mainly due to movements of the domain walls. As before, the local magnetic induction is not changed during magnetisation (19.1 kG). The film remains to be magnetically saturated when the applied field is decreased to 25 Oe. The magnetic texture of the film (17) as evaluated from γ_x is $\tau \geqslant 0.94$.

Such anisotropic film can be used to produce a spin turner (reflection mode) for monochromatic and collimated neutron beams [21]. Note that a similar device has been realised in the transmission mode [32].

The thicknesses of the film and the oxide layer were found from data fit to be equal to 169 ± 3 nm and 2 ± 1 nm, respectively.

5. Co film

Similar measurements were carried out with a Co film prepared by electron beam evaporation technique. The closeness of the hysteresis-like curves of P_{int} (Fig. 10) measured as a function of the applied field for two mutually perpendicular directions (1 and 2) shows that the magnetic film is almost isotropic. So, the other measurements were carried out only for sample orientation 1. The intensity of diffuse scattering I_{diff} summarised over the range of β from 3 to 12 mrad is also represented in Fig. 10. The profile of the reflected beam I_+ is given in Fig. 11 for two magnitudes of the field, when the film is demagnetised and magnetically saturated. An increase in the intensity of diffuse scattering near the demagnetised state can be explained by the appearance of small domains with dimensions less than the neutron coherence illumination length ($\delta < l_c$). The Fourier transform $K(q_\parallel)$ was approximated by the function $\exp(-q_\parallel \delta)$ [14]. The mean size δ of domains was evaluated to be about 3 μm (the curve in Fig. 11 is the fit). This evaluation is in agreement with the data obtained (SANS) for bulk samples [33]. The Yoneda wing in the diffuse scattering intensity (Fig. 11) is observed on the left side of the specular reflectivity peak (at smaller angles). Its position is connected with the Fresnel transmission coefficient

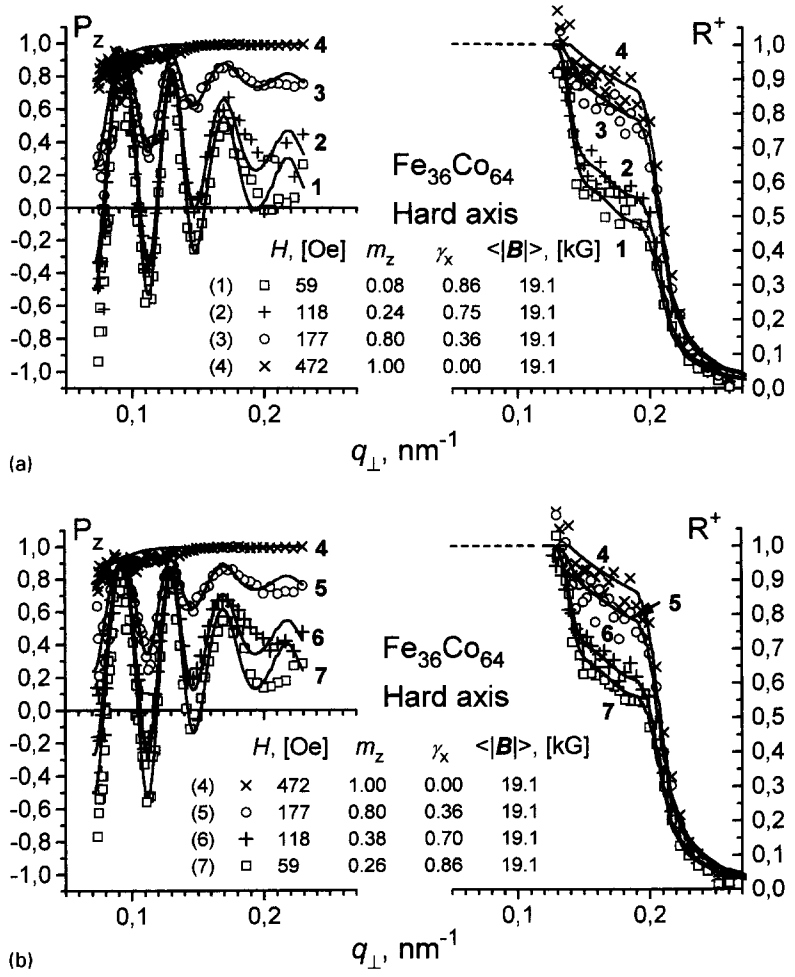

Fig. 8. The Z-component P_z of the polarisation vector of the reflected beam and the corresponding spin-up reflectivity R^+ for the $Fe_{36}Co_{64}$ film in different magnetic fields are given as functions of $q_\perp$ (points). The field applied along the hard axis is first increased (a) and then decreased (b). The solid curves correspond to calculations. The parameters of the domain structure (γ_x, m_z and $\langle|\boldsymbol{B}|\rangle$) for the corresponding magnetic fields are tabulated.

$|T(\beta)|$ [29], which is maximum when β is equal to the critical angle of total reflection θ_c. The angular dependence of diffuse scattering from magnetic materials is more complicated, since $|T(\beta)|$ is different for the opposite (up (+) and down (−)$\boldsymbol{B}$) spin components and the diffuse scattering has two Yoneda maxima at the angles $\beta = \theta_c^{\pm}$. It will lead to polarisation effects in diffuse scattering.

The quantities P_{int} measured as a function of the scattering angle β in different fields ($m_z = -0.80$, -0.24 and 0.98) are shown in Fig. 12. It is seen that the curves are antisymmetrical about the angular position of the specularly reflected beam, the degree of asymmetry being dependent on the mean magnetisation. The asymmetry is more conspicuous near the demagnetised state. When the magnetisation is reversed, the asymmetry changes its sign. The explanation of such a behaviour of P_{int} is made difficult by the circumstance that the measurements were carried out with a white neutron beam (no application of time-of-flight technique was done). The experiments

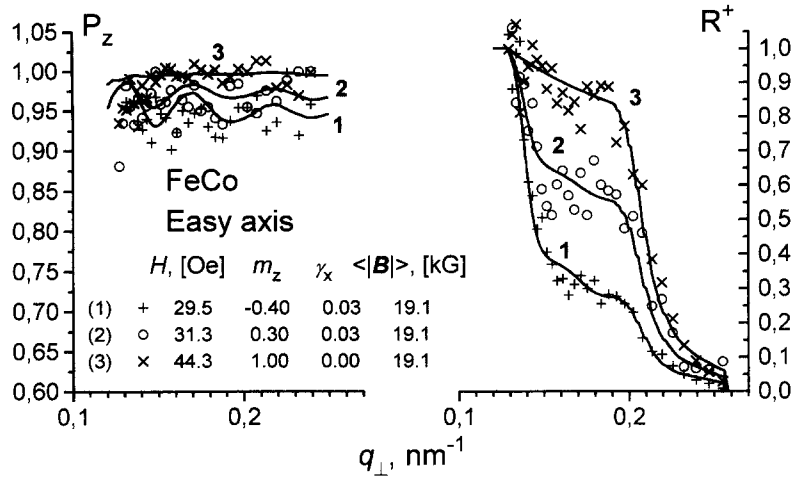

Fig. 9. The Z-component P_z of the polarisation vector of the reflected beam and the corresponding spin-up reflectivity R^+ for the $Fe_{36}Co_{64}$ film in different magnetic fields are given as functions of $q_\perp$ (points). The field applied along the easy axis is increased from 29.5 to 44.3 Oe. The solid curves correspond to calculations. The parameters of the domain structure (γ_x, m_z and $\langle \boldsymbol{B} \rangle$) for the corresponding magnetic fields are tabulated.

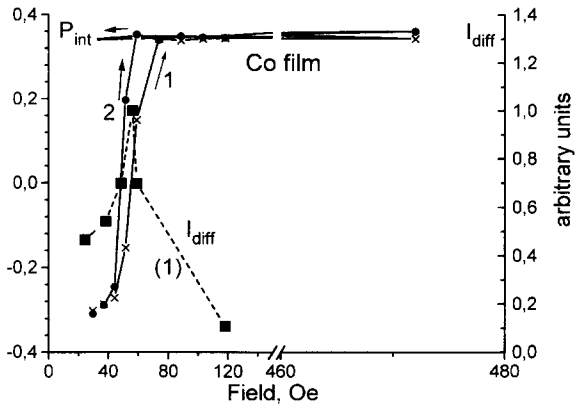

Fig. 10. The quantity P_{int} measured for a Co film for two mutually perpendicular directions (1) and (2), and the corresponding intensity of diffuse scattering I_{diff} (summarised over the range of β from 3 to 12 mrad) for direction (1) are represented as functions of the applied field (see also Fig. 11).

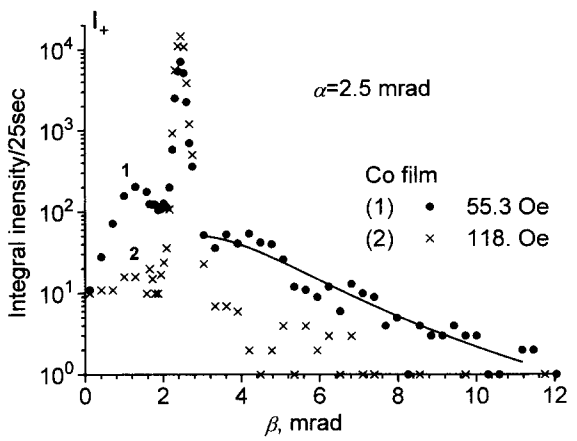

Fig. 11. The intensity I_+ of neutrons scattered from the demagnetised (curve 1) and magnetised (curve 2) Co film as a function of the scattering angle β. The dashed curve corresponds to the theoretical intensity of scattering at the domain structure with the mean size $\delta = 3$ μm. The glancing angle $\alpha = 2.5$ mrad.

will be continued in order to clarify this effect, too.

The appearance of small domains near the demagnetised state brings about a decrease in the local magnetic induction (from 15.9 to 13.3 kG), which is responsible for the shifts of extrema of P_z in the region of total reflection to smaller $q_\perp$ (Fig. 13). The magnitude of $\langle |\boldsymbol{B}| \rangle \neq 0$ testifies to the presence of large domains $\delta > l_c$. The mean size of large domains as evaluated by means of Eq. (14) from depolarisation of the beam reflected from

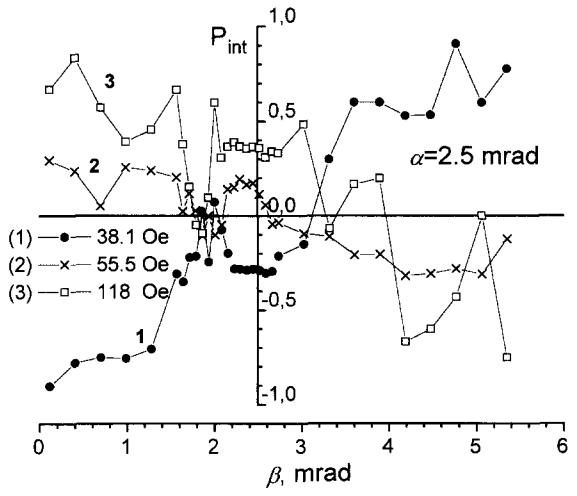

Fig. 12. The quantity P_{int} measured for a Co film in magnetic fields (1) 38.1, (2) 59.0, and (3) 118 Oe as a function of the scattering angle β. The field is applied along direction (1). The angle $\beta = 2.5$ mrad corresponds to the position of the specularly reflected beam.

a demagnetised ($m_z = -0.24$) film at $q_\perp \cong 0.14\ \mathrm{nm}^{-1}$ (curve 4 in Fig. 13) is ~ 150 μm. Such domains do not contribute to diffuse scattering from small domains, and the results obtained for small domains should not be corrected.

One may conclude from analysis of the parameters m_z and γ_x that rotation of magnetisation is accompanied by movements of domain boundaries. In our measurements the quantity γ_x is maximum and equal to 0.47 at $m_z = -0.66$. (Note that according to the definition of the texture parameter (17), the sample should be considered as magnetically isotropic even when the mean magnetisation is not zero; physically, it means that the distribution of the axes along which the domains are magnetised is isotropic, but the numbers of oppositely oriented domains do not coincide.) As a consequence, the amplitude of oscillations of P_z in the region of total reflection (see Eq. (11)) is maximum for this case (Fig. 13). The film is almost saturated ($\gamma_x = 0.04$, $m_z = 0.98$) in the field 118 Oe, and is slightly demagnetised when the field falls to 29.5 Oe ($\gamma_x = 0.10$, $m_z = 0.86$).

The optical effect of coherent averaging ($\delta \sim l_c$), which led to a decrease in the local magnetic induction of the film, was observed for the first time. In our case, l_c lies within the range 30–120 μm. It is to be noted that the effect of the instrument on the result of a quantum mechanical measurement has been discussed in connection with neutron reflection from the boundary of homogeneous magnetic media [21] and earlier in connection with small-angle neutron scattering at magnetic inhomogeneities [3]. Particularly, it was pointed out that neutron depolarisation in both cases may depend on the beam divergence. Note that the experimental verification of this conclusion cannot be easily done in transmission experiments. Such a possibility can be realised in our further experiments on reflection, since the length of the coherent illumination region is comparable to the mean size of magnetic domains and can be changed (at a given glancing angle) by changing the beam divergence or the neutron wavelength.

The thicknesses of the Co film and the oxide layer were found from data fit to be equal to 113 ± 2 nm and 4 ± 1 nm, respectively.

6. Conclusions

It may be concluded that specular reflection of polarised neutrons, complemented by polarisation analysis and small-angle (diffuse) scattering under reflection can be used for determination of parameters of domain structure of thin (~ 10–10^3 nm) films. The generalised matrix formalism developed to cope with the problem of reflection of neutrons from layered magnetic media with magnetisation arbitrary in magnitude and direction was found to be satisfactory for description of the specular reflection of neutrons from unmagnetised films, provided that the effect of neutron coherent averaging is taken into account. The optical effect of coherent averaging which led to a decrease in the 'local' (as 'seen' by neutrons) magnetic induction of a Co film have been observed for the first time. It is connected with the uncertainty relation for the neutron wavenumber component parallel to the surface.

The technique described may be useful for creation and development of neutron polarisers, memory and other devices on the basis of thin magnetic films.

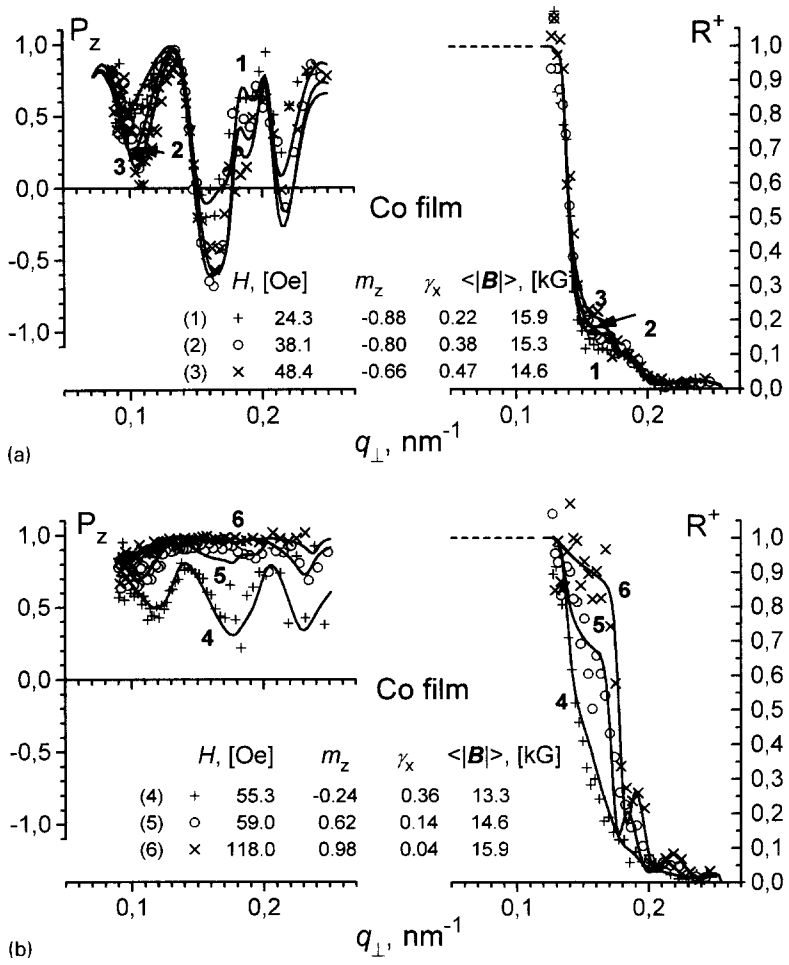

Fig. 13. The Z-component P_z of the polarisation vector of the reflected beam and the corresponding spin-up reflectivity R^+ for the Co film in different magnetic fields are given as functions of $q_\perp$ (points). The field applied along direction (1) is increased from 24.3 to 48.4 Oe (a) and further on up to 118 Oe (b). The solid curves correspond to calculations. The parameters of the domain structure (γ_x, m_z and $\langle|\boldsymbol{B}|\rangle$) for the corresponding magnetic fields are tabulated.

The study of magnetisation processes in $Fe_{36}Co_{64}$ (170 ± 3 nm) and Co (110 ± 3 nm) films demonstrates the possibilities of the new technique. It has been shown that the $Fe_{36}Co_{64}$ film prepared by magnetron sputtering possesses strong magnetic anisotropy, whereas the Co film prepared by thermal evaporation technique is practically isotropic. As it is to be expected, the magnetisation of the anisotropic $Fe_{36}Co_{64}$ film in the easy direction is only due to movements of domain boundaries. The magnetisation process in the hard direction is due to movements of domain boundaries, accompanied by rotation of the domain magnetisation. The movements of domain boundaries are always accompanied by rotation of the domain magnetisation in the Co film. It follows from analysis of experimental data that there are domains of two scales ~3 μm, and ~150 μm near the demagnetised state of the Co film.

To compare the possibilities of the new technique and to obtain an additional information about the films, magneto-optical and X-ray

measurements of $Fe_{36}Co_{64}$ and Co films are carried out presently. It has been found from X-ray diffraction measurements that $Fe_{36}Co_{64}$ and Co films are polycrystalline. It has been experimentally found also that the magnetic in-plane anisotropy of the $Fe_{36}Co_{64}$ film is related to the magnetron sputtering geometry. The direction of the anisotropy axis depends on the mean direction of motion of the particles in plasma, which are deposited onto the substrate during sputtering. Isotropy of the Co film is determined by symmetric planetary geometry used in the thermal evaporation technique.

The results of the present work have been partly represented at the 1st European Conference on Neutron Scattering (Interlaken, Switzerland, 1996) [34].

Acknowledgements

We wish to express our gratitude to B.G. Peskov, E.V. Siber, and Z.N. Soroko for preparation of the samples. This work was partially supported by the Russian Fund of Fundamental Research, Grant No. 96-02-18767.

References

[1] O. Halpern, T. Holstein, Phys. Rev. 59 (1941) 960.
[2] S.V. Maleyev, J. Phys. 43 (1982) C723.
[3] S.V. Maleyev, V.A. Ruban, JETP 58 (1970) 199.
[4] S.V. Maleev, V.A. Ruban, JETP 18 (8) (1976) 2283.
[5] M.Th. Rekveldt, Z. Phys. 259 (1973) 391.
[6] M.Th. Rekveldt, F.J. Schaik, J. Appl. Phys. 50 (3) (1979) 2122.
[7] B.P. Toperverg, J. Weniger, Z. Phys. B 74 (1989) 105.
[8] V.I. Sbitnev, Z. Phys. B 74 (1989) 321.
[9] W.H. Kraan, M.Th. Rekveldt, J.P.C. Bernards, S.B. Luitjens, J. Phys. C 8 (1988) 1981.
[10] O. Schaerpf, A. Bierfreund, H. Strothmann. J. Magn. Magn. Mater. 13 (1979) 243.
[11] S.Sh. Shilshteynn, V.A. Somenkov, M. Kalanov, Sov. Phys. JETP 63 (1972) 2214.
[12] S.Sh. Shilshteynn, N.O. Yelyutin, V.A. Somenkov, Sov. Phys. JETP 16 (1975) 1305.
[13] H. Strothmann, O. Schaerpf, J. Magn. Magn. Mater. 9 (1978) 257.
[14] V.I. Mikerov, A.V. Vinogradov, I.V. Kozhevnikov, F.A. Pudonin, V.A. Tukarev, M.P. Yakovlev, Physica B 174 (1991) 174.
[15] G.P. Felcher, Phys. Rev. B 24 (1981) 1595.
[16] O. Schaerpf, J. Appl. Crystallogr. 11 (1978) 626.
[17] G.P. Felcher, R.O. Hilleke, R.K. Crawford, J. Haumann, R. Kleb, G. Ostrowski, Rev. Sci. Instrum. 4058 (1987) 609.
[18] Ch.F. Majkrzak, Physica B 156&157 (1989) 619.
[19] D.A. Korneev, L.P. Chernenko, Neutron Optical Devices and Applications, in: Ch.F. Majkrzak, J.L. Wood (Eds.), Proc. SPIE, vol. 1738, 1992, p. 468.
[20] S.J. Blundell, J.A. Bland, Phys. Rev. B 46 (1992) 3391.
[21] N.K. Pleshanov, Z. Phys. B 94 (1994) 233.
[22] N.K. Pleshanov, V.M. Pusenkov, A.F. Schebetov, B.G. Peskov, G.E. Shmelev, E.V. Siber, Z.N. Soroko, Physica B 198 (1994) 27.
[23] N.K. Pleshanov, Z. Phys. B 100 (1996) 423.
[24] N.K. Pleshanov, V.M. Pusenkov, Z. Phys. B 100 (1996) 507.
[25] N.K. Pleshanov, Physica B 198 (1994) 70.
[26] H. Zabel, Physica B 198 (1994) 156.
[27] V.Ya. Kezerashvili, Dissertation, LNPI, 1986.
[28] S.K. Sinha, E.B. Sirota, B. Garoff, H.B. Stanley, Phys. Rev. B 38 (1988) 2297.
[29] S.K. Sinha, Acta Phys. Polon. A 89 (1996) 216.
[30] Y.P. Feng, S.K. Sinha, C.A. Melendres, D.D. Lee, Physica B 221 (1996) 251.
[31] V. Syromyatnikov, B. Toperverg, V. Deriglazov, A.F. Schebetov, T. Ebel, R. Kampman, R. Wagner, Physica B 234–236 (1997) 475.
[32] L.A. Akselrod, G.P. Gordeev, I.M. Lazebnik, V.T. Lebedev, Preprint LNPI 883 Leningrad, 1983.
[33] R. Lermer, A. Steyerl, Phys. Stat. Sol. (a) 33 (1976) 531.
[34] V.M. Pusenkov, N.K. Pleshanov, V.G. Syromyatnikov, V.A. Ul'yanov, A.F. Schebetov, Physica B 234–236 (1997) 519.